Water Research X 24 (2024) 100243

Contents lists available at ScienceDirect

Water Research X

journal homepage: www.sciencedirect.com/journal/water-research-x

Carbon footprint analysis of wastewater treatment processes coupled with sludge in situ reduction

Yiyue Sun [a], Yi Zuo [a], Yanjun Shao [a], Lihua Wang [b], Lu-Man Jiang [a], Jiaming Hu [a], Chuanting Zhou [c], Xi Lu [d], Song Huang [d], Zhen Zhou [a,*]

[a] Shanghai Engineering Research Center of Energy - Saving in Heat Exchange Systems, College of Environmental and Chemical Engineering, Shanghai University of Electric Power, Shanghai 200090, China
[b] Shanghai Chengtou Wastewater Treatment Co., Ltd, Shanghai 201203, China
[c] Shanghai Urban Construction Design and Research Institute, Shanghai 200125, China
[d] Shanghai Investigation Design and Research Institute Co., Ltd, Shanghai 200335, China

ARTICLE INFO

Keywords:
Sludge in situ reduction (SIR)
Carbon emission
Greenhouse gas (GHG)
Sludge process reduction activated sludge process (SPRAS)
Anaerobic side-stream reactor (ASSR)

ABSTRACT

The goal of this study was to assess the impacts or benefits of sludge in situ reduction (SIR) within wastewater treatment processes with relation to global warming potential in wastewater treatment plants, with a comprehensive consideration of wastewater and sludge treatment. The anaerobic side-stream reactor (ASSR) and the sludge process reduction activated sludge (SPRAS), two typical SIR technologies, were used to compare the carbon footprint analysis results with the conventional anaerobic - anoxic - oxic (AAO) process. Compared to the AAO, the ASSR with a typical sludge reduction efficiency (SRE) of 30 % increased greenhouse gas (GHG) emissions by 1.1 - 1.7 %, while the SPRAS with a SRE of 74 % reduced GHG emissions by 12.3 - 17.6 %. Electricity consumption (0.025 - 0.027 kg $CO_{2\text{-eq}}/m^3$), CO_2 emissions (0.016 - 0.059 kg $CO_{2\text{-eq}}/m^3$), and N_2O emissions (0.009 - 0.023 kg $CO_{2\text{-eq}}/m^3$) for the removal of secondary substrates released from sludge decay in the SIR processes were the major contributor to the increased GHG emissions from the wastewater treatment system. By lowering sludge production and the organic matter content in the sludge, the SIR processes significantly decreased the carbon footprints associated with sludge treatment and disposal. The threshold SREs of the ASSR for GHG reduction were 27.7 % and 34.6 % for the advanced dewatering - sanitary landfill and conventional dewatering - drying-incinerating routes, respectively. Overall, the SPRAS process could be considered as a cost-effective and sustainable low-carbon SIR technology for wastewater treatment.

Introduction

Wastewater treatment plants (WWTPs) were one of the major sources of greenhouse gases (GHGs) emissions (Lu et al., 2018), and contributed around 3 % of the global GHG emissions (Samuelsson et al., 2018). The emissions of carbon dioxide (CO_2), methane (CH_4), and nitrous oxide (N_2O) accounted for the largest proportion, leading them to the prior targets when evaluating the GHGs characteristics in WWTPs (Huang et al., 2020). Stricter discharge standards imposed on WWTPs in recent years have increased energy usage and GHG emissions (Gu et al., 2016). In addition, the treatment and disposal of waste activated sludge (WAS) generate 25 - 65 % of the total operating cost of WWTPs (Nayeb et al., 2019; Zhou et al., 2014a) and 40 % of GHG emissions produced by WWTPs (Brown et al., 2010). Increasing sludge yield was the main driver of GHG emissions from WWTPs after 2015 with the implementation of stricter discharge standards in China; as a result, sludge reduction has become crucial for controlling GHG emissions across the country (Chen et al., 2022; Huang et al., 2023). Nevertheless, previous

Abbreviations: AAO, Anaerobic - anoxic - oxic; AD, Advanced dewatering; ASSR, Anaerobic side-stream reactor; BOD, Biological oxygen demand; CH_4, Methane; CO_2, Carbon dioxide; COD, Chemical oxygen demand; CD, Conventional dewatering; CS, Chemical sludge; HRT, Hydraulic retention time; k_d, Endogenous decay constant; N_2O, Nitrous oxide; TP, Total phosphorus; WAS, Waste activated sludge; NH_4^+-N, Ammonia nitrogen; N/DN, Nitrification and denitrification; PAC, Poly aluminum chloride; PAM, Polyacrylamide; SIR, Sludge in situ reduction; SPRAS, Sludge process reduction activated sludge; SRT, Solids retention time; SL, Sanitary landfill; SS, Suspended solids; TN, Total nitrogen; DS, Dry sludge; DI, Drying-incineration; EF, Emission factor; GHG, Greenhouse gas; WWTP, Wastewater treatment plant; Y_{obs}, Observed sludge yield.

* Corresponding author.
E-mail address: zhouzhen@shiep.edu.cn (Z. Zhou).

https://doi.org/10.1016/j.wroa.2024.100243
Received 30 April 2024; Received in revised form 3 July 2024; Accepted 23 July 2024
Available online 25 July 2024

literatures of GHG emissions usually focused on wastewater treatment systems and sludge terminal treatment and disposal; it has not, however, examined the functions of sludge reduction in WWTPs through a systematic evaluation (Chen et al., 2022).

Sludge in situ reduction (SIR) is promising as it can reduce sludge production within wastewater treatment processes rather than struggling with its terminal treatment and disposal (Niu et al., 2016). Two promising SIR processes that have been used in full-scale WWTPs are the anaerobic side-stream reactor (ASSR) and the sludge process reduction (SPR) activated sludge (SPRAS) processes (Shao et al., 2022; Wang et al., 2013). The ASSR process has been applied in the Levico WWTP (Italy) with capacity of 10,000 m^3/d (Velho et al., 2016) and a municipal WWTP (Italy) of 5000 m^3/d (Ferrentino et al., 2019), while the SPRAS in an industrial park WWTP (China) of 20,000 m^3/d (Jiang et al., 2018). By adding an anaerobic reactor to the return activated sludge line, the ASSR reduced sludge production by 18.3 - 50.5 % (Ferrentino et al., 2019; Zhou et al., 2015a). The SPRAS was a two-sludge system that achieved substantially higher sludge reduction efficiency (SRE) of 57.9 - 76.6 % by inserting an SPR unit, which consisted of a microaerobic tank and an SPR settler, prior to the activated sludge process (Niu et al., 2016; Zhou et al., 2023). The SIR process effectively decreased sludge production and the associated GHG emissions from sludge treatment and disposal. However, it necessitated the use of external reaction space, energy, and chemicals for sludge reduction and phosphorus removal, which likely increased the emissions of GHGs from sludge degradation as well as indirect emissions from energy and chemical consumption. It is of great significance to compare GHG emissions between conventional wastewater treatment process and SIR process systematically to evaluate the benefits of SIR technology on GHGs reduction and identify the low-carbon process.

The goal of this study is to assess and compare the carbon footprint, including direct (CO_2, CH_4, and N_2O) and indirect GHG emissions, produced in a hypothetical WWTP with a treatment capacity of 100,000 m^3/d using the conventional anaerobic - anoxic - oxic (AAO), ASSR or SPRAS processes (Fig. 1a-1c). The sludge reduction and pollutants removal of ASSR and SPRAS were evaluated based on two full-scale WWTPs, respectively. Carbon footprint analysis on various combinations of wastewater and sludge treatment and disposal technologies was carried out by gathering data and setting parameters to create scenarios to understand the contribution of different sectors to GHG emissions and identify the primary hotspots under various conditions. Moreover, impact of SRE on carbon footprints was explained to demonstrate the viability of SIR processes. This study would shed new light on possible SIR process for achieving low-carbon wastewater treatment with low sludge yield.

Results and discussion

Wastewater treatment performance

The full-scale ASSR WWTPs obtained efficient COD removal with the concentration in the effluent of 22.0 ± 3.9 mg/L in spite of the wide variation in the influx COD from 178 - 642 mg/L (Fig. S1a). The ASSR also achieved a very high nitrification efficiency (99.5 %), yielding the concentration of NH_4^+-N in the effluent of 0.12 ± 0.17 mg/L (Fig. S1b). The average TN concentrations in the influent and effluent were 46.2 ± 15.2 and 6.4 ± 1.9 mg/L, yielding a high removal efficiency of 85.6 % (Fig. S1c). Efficient nitrogen removal was attributed to three reasons, high nitrate recirculation, simultaneous nitrification and denitrification in the membrane bioreactor (MBR) tank with high sludge concentration (> 15 g/L), and enhanced denitrification with released secondary substrate from ASSR. Previous literatures also confirmed that nitrogen removal efficiency was significantly elevated in the ASSR because dissolved organic matters released from particles hydrolysis and cell lysis were utilized by denitrifiers (Zheng et al., 2019a; Zhou et al., 2015a). The low TP concentration (0.09 ± 0.03 mg/L) was confirmed by chemical precipitation of effluent from the ASSR-MBR process (Fig. S1d).

For the full-scale SPRAS WWTPs (Fig. S2), the average COD concentrations in the influent and effluent were 345.4 ± 22.2 and 25.8 ± 5.1 mg/L, yielding a high removal efficiency of 91.7 %. Efficient nitrification (99.4 %) was achieved in the SPRAS with NH_4^+-N concentrations in the effluent of 0.20 ± 0.19 mg/L. The WWTPs obtained an average nitrogen removal efficiency of 68.9 % via simultaneous nitrification and denitrification in the micro-aerobic tank and denitrification in the anoxic zone (Jiang et al., 2018; Shao et al., 2022), with effluent TN concentrations (11.30 ± 2.09 mg/L) satisfying the requirements of GB 18,918–2002. The SPRAS usually deteriorated TP removal because of its low WAS discharge (Niu et al., 2016), while the chemical precipitation in the effluent of SPRAS confirmed low TP concentrations (0.23 ± 0.09 mg/L) in the full-scale WWTP.

Based on full-scale data mentioned above, pollutants concentrations in the influent and effluent of three hypothetical WWTPs are given in combination of reported lab-and pilot-scale data (Table 1) (Cheng et al., 2017; Jiang et al., 2021, 2018; Shao et al., 2022; Zheng et al., 2019b). All three systems performed comparably well in the removal of COD and NH_4^+-N, with average removal efficiencies of > 88 % and 97 %, respectively. It appears that the SIR process did not impair the ability of organic matter degradation and nitrification (Zheng et al., 2019b). The ASSR (77.8 %) obtained higher TN removal efficiency than the AAO (73.3 %) because sludge decay in the ASSR provided more internal carbon source for denitrification (Cheng et al., 2017), while the SPRAS (70.2 %) decreased the efficiency due to the degradation of influent COD in the microaerobic tank (Shao et al., 2022). Due to the low sludge discharge in the SIR processes, ASSR and SPRAS had greater TP concentrations in the effluent than the AAO (Jiang et al., 2021). On the other hand, the ASSR with single-sludge configuration and lengthy SRT often resulted in higher SS concentrations in the effluent (Cheng et al., 2017), while the two-sludge configuration of the SPRAS could ensure efficient solid-liquid separation in the secondary clarifier (Jiang et al., 2018). By adding aluminum or iron salts, the TP and SS in the downstream coagulation-settling tank can be reduced to a low level.

Sludge reduction performance

The wastewater treatment structures in the red dashed line in Fig. 2a and 2b are the ASSR and SPR module for sludge reduction in two full-scale SIR WWTPs. The average observed sludge yield (Y_{obs}) value in the ASSR and SPRAS WWTPs were calculated at 0.245 ± 0.017 and 0.092 ± 0.031 kg SS/kg COD without obvious seasonal variations (Fig. 2c). The calculated Y_{obs} values of two full-scale WWTPs were in the typical range of ASSR (0.111 - 0.600 kg SS/kg COD) and SPRAS (0.069 - 0.103 kg SS/kg COD) (Shao et al., 2022; Velho et al., 2016; Zheng et al., 2019a; Zhou et al., 2014a; Zhou et al., 2023). Anaerobic hydrolysis and maintenance metabolism reduced sludge production in the ASSR, while accelerated hydrolysis by micro-aeration, metabolic uncoupling, and greatly prolonged solids retention time (SRT) of the overall system induced higher sludge reduction in the SPRAS (Niu et al., 2016; Shao et al., 2022).

The Y_{obs} values of conventional activated sludge processes ranged from 0.27 to 0.44 kg SS/kg COD (Huang et al., 2019; Velho et al., 2016). In this study, the Y_{obs} of the AAO process was set at 0.350, 0.245, and 0.092 kg SS/kg COD, and SREs of ASSR and SPRAS processes were 30 % and 74 %, which were also in the reported typical range (Ferrentino et al., 2019; Niu et al., 2016; Zhou et al., 2023; Zhou et al., 2015a). The obvious sludge decay in the ASSR and SPRAS resulted in the release of nitrogen and phosphorus, which should be taken into the influent characteristics for computation, with default values of 40 mg N and 20 mg P per gramme suspended solids (SS) (Huang et al., 2020). To assess the GHG emissions from the sludge decay process, the endogenous decay constant (k_d) was chosen for different reactors. The k_d of the ASSR and the SPR units were 0.06 and 0.12 d^{-1}, while the k_d values of the other

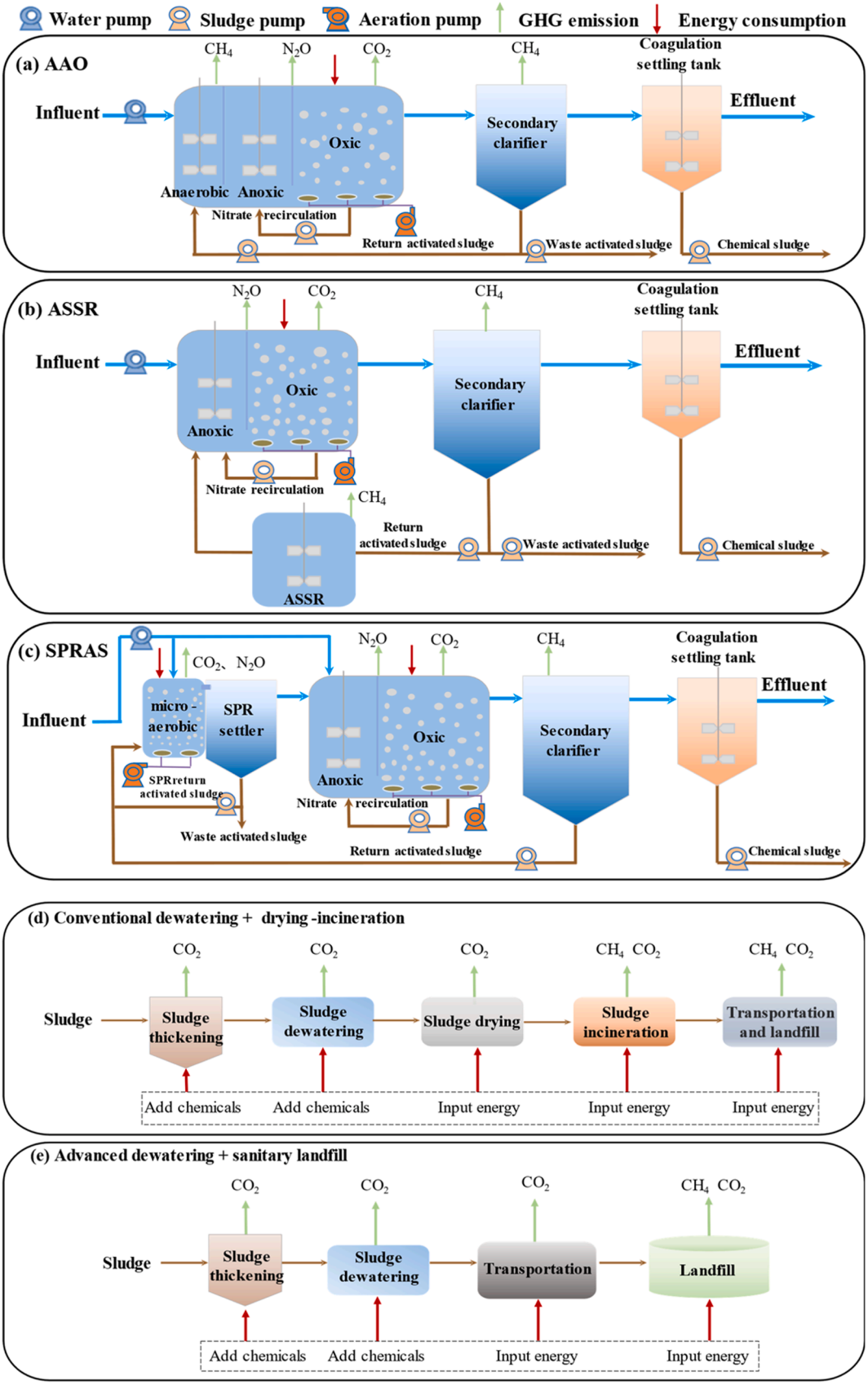

Fig. 1. Scenarios and boundary of wastewater management approach in this study. Wastewater treatment process flow chart of (a) AAO, (b) ASSR, and (c) SPRAS; sludge treatment and disposal route of (d) conventional dewatering + drying-incineration and (e) advanced dewatering + sanitary landfill. The sludge and water lines are blue and brown, respectively. Red arrows indicate the use of chemicals and electricity, while green arrows show GHG emissions.

Table 1
Characteristics of influent and effluent of AAO, ASSR, and SPRAS processes (mg/L).

Index		COD	BOD_5	SS	NH_4^+-N	TN	TP
Influent		360	160	140	40	45	5
Effluent of secondary clarifier	AAO	35	5	15	1.0	12	1
	ASSR	40	10	30	1.0	10	2
	SPRAS	35	5	15	1.0	13	3
Final effluent		25	5	8	1.0	10 - 13	0.3
Discharge standard		50	10	10	5	15	0.5

units were the same as that of the AAO (0.05 d^{-1}) (Shao et al., 2022).

Carbon footprint comparison of AAO and SIR processes

Two sludge treatment and disposal routes, the conventional dewatering (CD) + drying-incineration (DI) (CD/DI route) and advanced dewatering (AD) + sanitary landfill (SL) (AD/SL route), were combined with the three wastewater treatment processes to create six scenarios: AAO - CD/DI, AAO - AD/SL, ASSR - CD/DI, ASSR - AD/SL, SPRAS - CD/DI, and SPRAS - AD/SL. GHG emissions ranged from 0.76 to 1.09 kg $CO_{2\text{-eq}}/m^3$ for six scenarios (Fig. 3), and within the range of WWTPs (0.75 to 1.25 kg $CO_{2\text{-eq}}/m^3$) presented in Pagilla et al. (2009). The GHG emissions from ASSR grew by 1.7 % and 1.1 % under the CD/DI and AD/SL routes, respectively, in comparison to AAO, while the emissions of SPRAS reduced by 17.6 % and 12.3 %. The GHG emissions of the wastewater treatment systems of AAO, ASSR, and SPRAS were 0.56, 0.64, and 0.67 kg $CO_{2\text{-eq}}/m^3$, respectively (Fig. 3).The GHG emissions of other wastewater treatment systems were reported in the range of 0.54 to 0.82 kg $CO_{2\text{-eq}}/m^3$ (Flores-Alsina et al., 2011). The GHG emissions from the wastewater treatment system were comparable between the two SIR processes, and significantly higher than AAO. The primary cause of the increased GHG emissions was the removal of organic and nitrogenous materials released from sludge decay. This led to higher direct emissions (0.043 - 0.076 kg $CO_{2\text{-eq}}/m^3$) and additional aeration energy (0.025 - 0.027 kg $CO_{2\text{-eq}}/m^3$). With sludge yields of 12.8, 11.2, and 5.2 t DS/d in the AAO, ASSR, and SPRAS, the GHG emissions of the CD/DI route were 0.512, 0.459, and 0.219 kg $CO_{2\text{-eq}}/m^3$, and those of the AD/SL route were 0.299, 0.237, and 0.088 kg $CO_{2\text{-eq}}/m^3$, which were 42 - 60 % lower than the CD/DI route, respectively. Low sludge yield in the SIR process decreased the GHG emissions in the sludge treatment and disposal process, which offset energy consumption and direct GHG emissions in the wastewater treatment system. The results indicated that the SPRAS has the highest GHG emissions reduction potential among the three processes.

Emissions from the wastewater treatment process

Direct emissions

In the AAO, direct GHG emissions from the wastewater treatment system accounted for 37.8 - 47.2 % of total emissions; in the ASSR and SPRAS, this percentage rose to 41.1 - 51.6 % and 54.4 - 63.8 %, respectively (Fig. 4). The SPRAS had the highest direct GHG emissions (0.483 kg $CO_{2\text{-eq}}/m^3$), followed by the ASSR (0.451 kg $CO_{2\text{-eq}}/m^3$) and AAO (0.408 kg $CO_{2\text{-eq}}/m^3$). Both CO_2 and N_2O were mainly emitted to the atmosphere from biological units (Bani Shahabadi et al., 2009), and the contribution rates of CO_2 and N_2O to the total direct GHG emissions were 39.7 - 48.8 % and 51.2 - 60.3 %, respectively.

N_2O emissions from the N/DN process contributed the most to the total emissions (22.8 - 32.9 %), and about 93.1 % of N_2O was generated

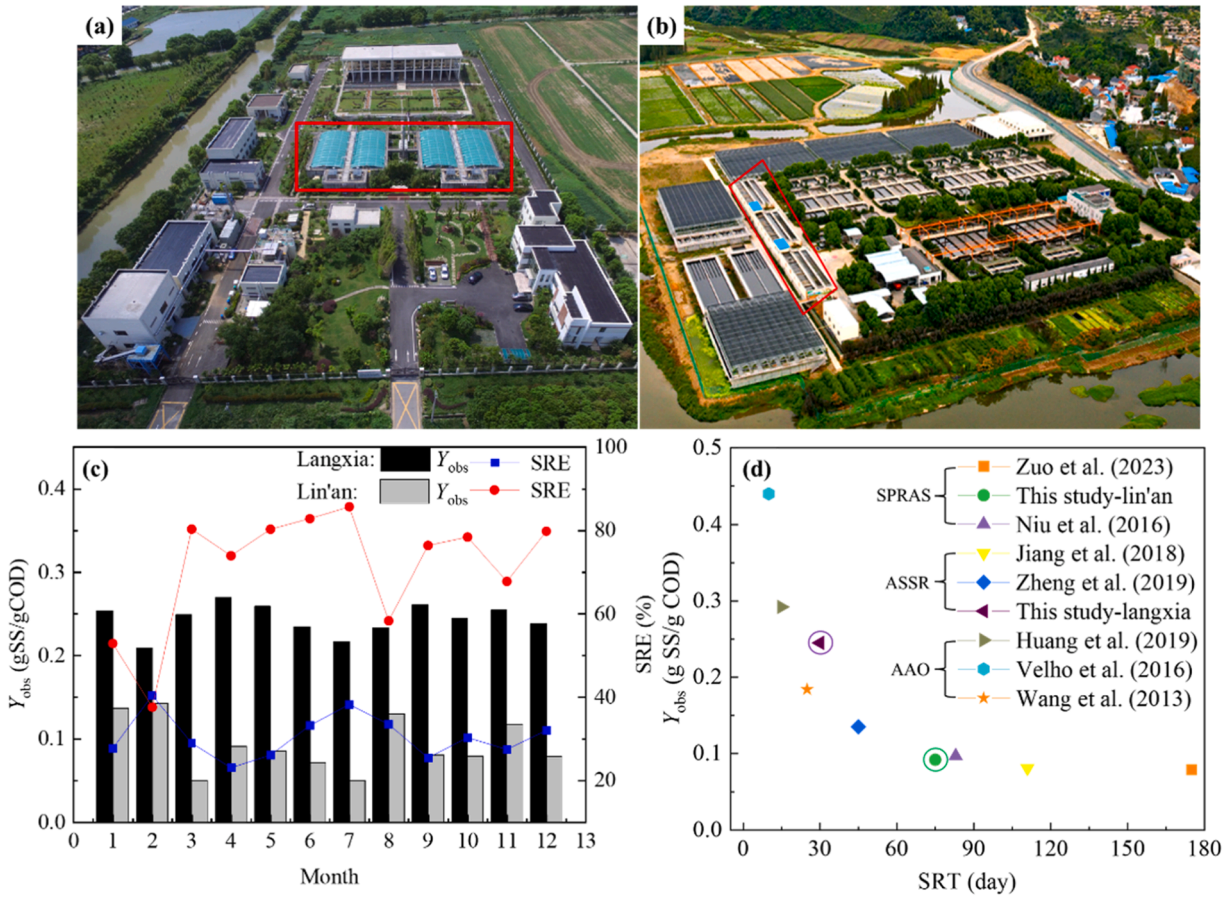

Fig. 2. Aerial view of full-scale ASSR (a) and SPRAS (b) WWTPs, and their observed sludge yield (c and d).

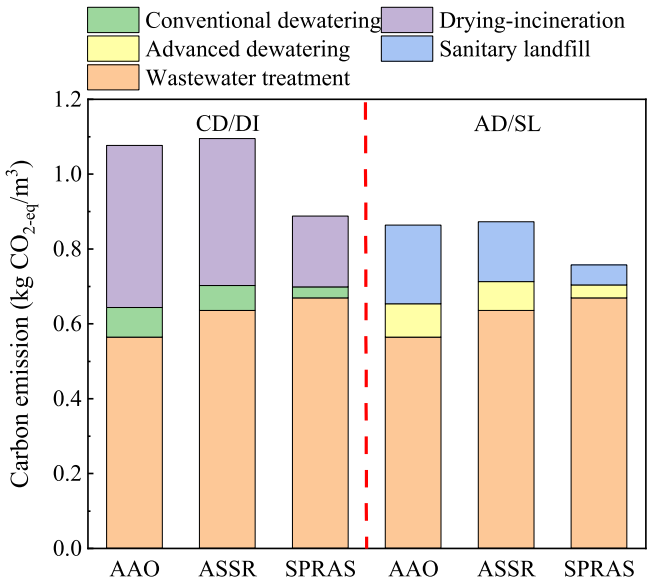

Fig. 3. GHG emissions throughout the process of AAO, ASSR, and SPRAS.

from the denitrification process according to the model proposed by Mannina et al. (2019), which was because nitrifier denitrification is the dominant pathway of N_2O in the N/DN process (Foley et al., 2010; Li et al., 2023). Due to the release of secondary substrate and the enrichment of nitrifying bacteria (Jiang et al., 2021), inserting ASSR greatly improved denitrification (Table 1); as a result, N_2O emissions in the ASSR increased by 9.4 % when compared to AAO. When taking into account the nitrogen species released from the sludge decay, the actual nitrogen removal in SPRAS (35.1 mg/L) was higher than that in AAO (33.0 mg/L), even though the nitrogen removal efficiency decreased in SPRAS due to the significant consumption of COD in the SPR module (Niu et al., 2016; Shao et al., 2022). Lastly, there was a 3.6 % rise in N_2O emissions in SPRAS. In addition to consuming CO_2 (EF of −0.308 kg $CO_{2\text{-eq}}$/kg N), the nitrification process also generates N_2O (0.513 kg $CO_{2\text{-eq}}$/kg N), which eventually raises GHG emissions. The GHG emissions resulting from nitrification in AAO, ASSR, and SPRAS were 0.0068, 0.0074, and 0.0070 kg $CO_{2\text{-eq}}/m^3$, respectively. These emissions were strongly linked to the release of nitrogen from the SIR process (Cheng et al., 2017).

The second contributor to direct emissions was CO_2 emissions (Fig. 4). GHG emissions from sludge decay increased by 0.016 and 0.059 kg $CO_{2\text{-eq}}/m^3$ in ASSR and SPRAS, which was negatively correlated with Y_{obs}. The process of organic matter oxidation was positively related to the removal rate of BOD, leading to three comparable GHG emissions of 0.084, 0.088, and 0.091 kg $CO_{2\text{-eq}}/m^3$ in AAO, ASSR, and SPRAS, respectively. The higher GHG emissions from organic matter oxidation were attributed to the longer SRT in two SIR systems.

Indirect emissions

Energy consumption of the wastewater treatment system was 0.27 - 0.31 kWh/m^3 in the three processes, and was close to the reported average value of 0.3 kWh/m^3 (Bani Shahabadi et al., 2010). The indirect emissions from the energy consumption accounted for 14.4 - 23.7 % (0.156 - 0.183 kg $CO_{2\text{-eq}}/m^3$) of the total emissions. Aeration accounted for 55.0 %, 46.6 %, and 44.6 % of the overall energy consumption of wastewater treatment in SPRAS, ASSR, and AAO, respectively. SIR processes released extra COD and NH_4^+-N due to sludge decay (Cheng et al., 2017), which requires more energy to oxidize. Extra energy was also required in SPRAS to maintain a microaerobic environment in the SPR, but this increase in energy consumption was not significant. It was because compared to the conventional aerobic state, micro-aeration had a higher oxygen mass transfer driving force and oxygen utilization rate (Fan et al., 2017). Ultimately, the ASSR and SPRAS increased energy consumption by 0.025 and 0.027 kg $CO_{2\text{-eq}}/m^3$, respectively. Chemicals made up 0.2 - 0.5 % of the total emissions of the wastewater treatment system. More chemicals were required to remove phosphorus in the SIR processes, and ASSR also needed extra coagulant to remove SS from the effluent (Cheng et al., 2017).

Emissions from the sludge treatment and disposal system

In the CD/DI route, the GHG emissions of the CD stage were 0.079, 0.066 and 0.030 kg $CO_{2\text{-eq}}/m^3$ in AAO, ASSR and SPRAS (Fig. 3), which were not directly proportional to sludge yields because higher amount of conditioner was required to dewater sludge with a higher VSS/SS ratio (Wu et al., 2019). The DI stage was the primary source of GHG emissions, and mainly consists of drying, coal consumption, electricity consumption, N_2O and CH_4 emissions generated from incomplete combustion, incineration ash transportation and landfills, and carbon offsets from energy recovery from sludge (Wei et al., 2020). In the DI stage, coal consumption emissions contributed the most (0.100 - 0.240 kg $CO_{2\text{-eq}}/m^3$), followed by sludge drying (0.094 - 0.234 kg $CO_{2\text{-eq}}/m^3$). Both contributions were directly related to the sludge production. The remaining processes only accounted for 22.3 - 23.4 % of the total emissions in the DI stage. Because sludge has an average calorific value of 4.8 MJ/kg VSS (Menéndez et al., 2002), the carbon offsets produced by heat recovery of sludge incineration were −0.095, −0.073, and −0.024 kg $CO_{2\text{-eq}}/m^3$ in AAO, ASSR, and SPRAS.

In the AD/SL route, the GHG emissions in the AD stage were 0.089, 0.076 and 0.035 kg $CO_{2\text{-eq}}/m^3$, respectively, with the similar trend as those in the CD stage. GHG emissions in the SL stage (0.054 - 0.210 kg $CO_{2\text{-eq}}/m^3$) mainly includes the release of CH_4 and N_2O, and dewatered sludge transportation. The predominant contributor was CH_4 released from landfills (0.052 - 0.205 kg $CO_{2\text{-eq}}/m^3$) because CH_4 is not only released in quantity but has a high global warming potential (Flores-Alsina et al., 2014). The N_2O release from landfills and the GHG emissions generated during transportation were 0.001 - 0.002 and 0.001 - 0.003 kg $CO_{2\text{-eq}}/m^3$.

Carbon footprint evaluation of the SIR processes

GHG emissions of two SIR processes have a near linear relationship with SRE (Fig. 5) because they majorly depend on the EF difference between the SIR process and the sludge treatment and disposal process. The total GHG emissions of ASSR were higher than the reference level at low SREs, then decreased with the rising SREs, and ultimately fell below the reference level (AAO) when SREs exceeded a threshold value (Fig. 5a). The threshold value of the ASSR were 27.7 % and 34.6 % for the AD/SL and CD/DI routes, respectively. The results indicated that although the ASSR and its deviated processes have been intensively investigated in recent years, their GHG emissions were still higher than the conventional processes because SREs of the ASSR were lower than 30 % in most cases (Jiang et al., 2021). Regulating hydraulic retention times (HRTs) of the side-stream reactor and the side-stream ratio were two effective measures to maximize SREs in the ASSR system (Cheng et al., 2017; Jiang et al., 2021). Packing carriers, feeding influent wastewater, and switching between the anaerobic and micro-aerobic states have all been shown to be successful in raising SREs to above 40 % in the ASSR (Zheng et al., 2019b). These strategies were critical and sustainable for the ASSR process from the perspective of comprehensive carbon footprint analysis. The SPRAS process was a low-carbon wastewater treatment technique; in the typical range of SREs (Fig. 5b), its total GHG emissions were 8.3 - 11.3 % and 13.0 - 18.7 % lower than the AAO process for the AD/SL and CD/DI routes, respectively. Maintaining the micro-aerobic state and extending HRT of the intermediate clarifier were crucial tactics in the SPRAS system to guarantee high SRE (Niu et al., 2016; Zhou et al., 2023).

Sludge reduction within the activated sludge process was considered as one of the first priorities in the cleaner production hierarchy of municipal WWTPs (Cheng et al., 2018). Only the SPRAS with high SRE

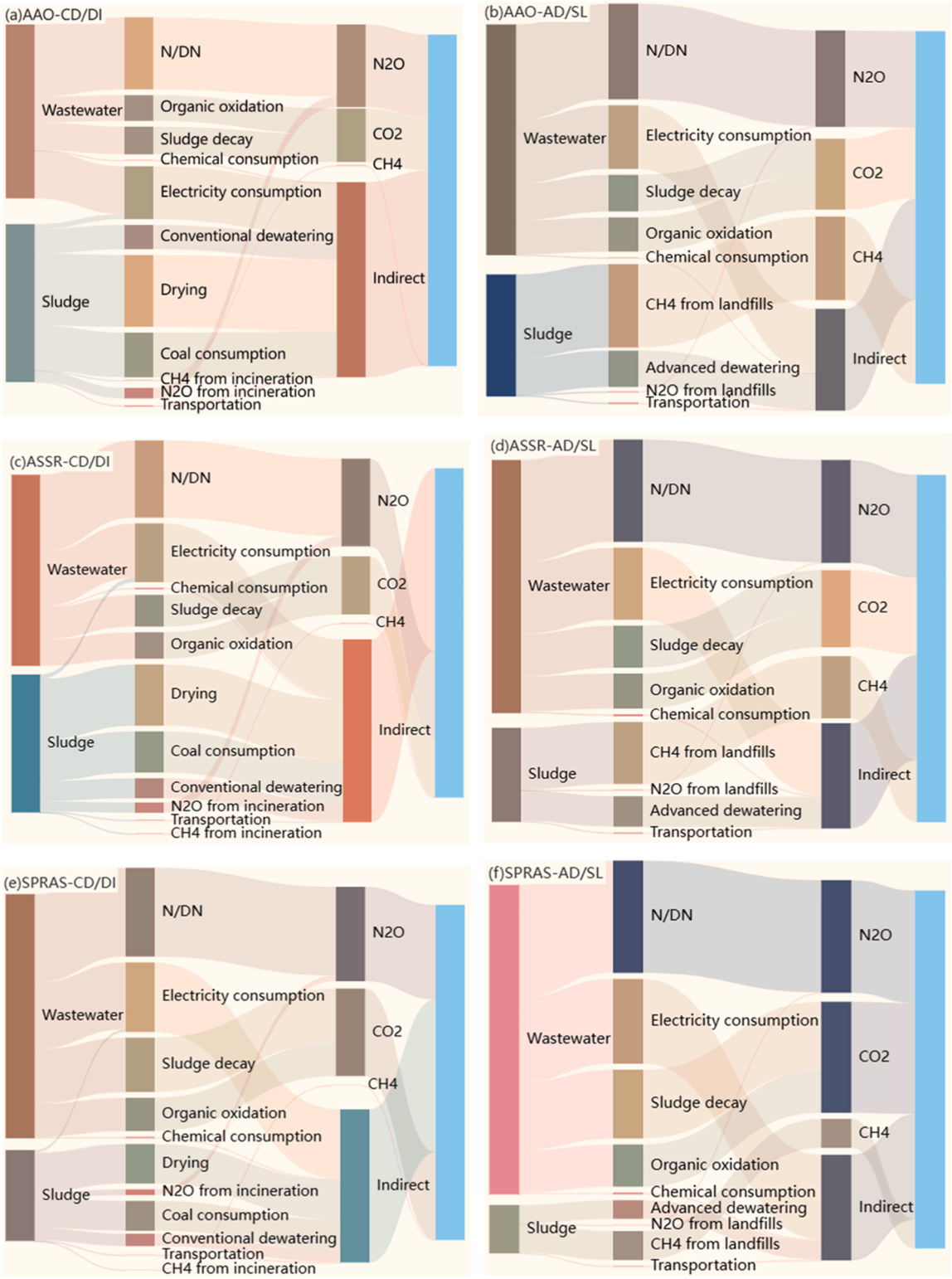

Fig. 4. GHG distribution of the six scenarios throughout the process of AAO, ASSR, and SPRAS. The proportion is accounted for by kg $CO_{2\text{-eq}}/m^3$.

and low energy input demonstrated a clear potential for reducing carbon emissions; the SIR processes with low SRE, on the other hand, had no advantages in this regard. Sludge reduction within the activated sludge process greatly elevated GHG emissions of the wastewater treatment system because of the increased energy consumption to oxidize released secondary substrates and directed emissions (CO_2 and N_2O). As a result, the combination of SIR with resource recovery has good prospects for carbon emission reduction, such as utilizing secondary substrate for methane production, or ammonium ion exchange and nitrogen recovery from the effluent of the SPR module to reduce N_2O discharge (Qin et al., 2023). The physicochemical SIR methods, such as ultrasonication, ozonation, and ferrate oxidation (An et al., 2017; Torregrossa et al., 2012; Zheng et al., 2019a), usually consumes greatly higher energy than biological SIR processes, and should be combined with more

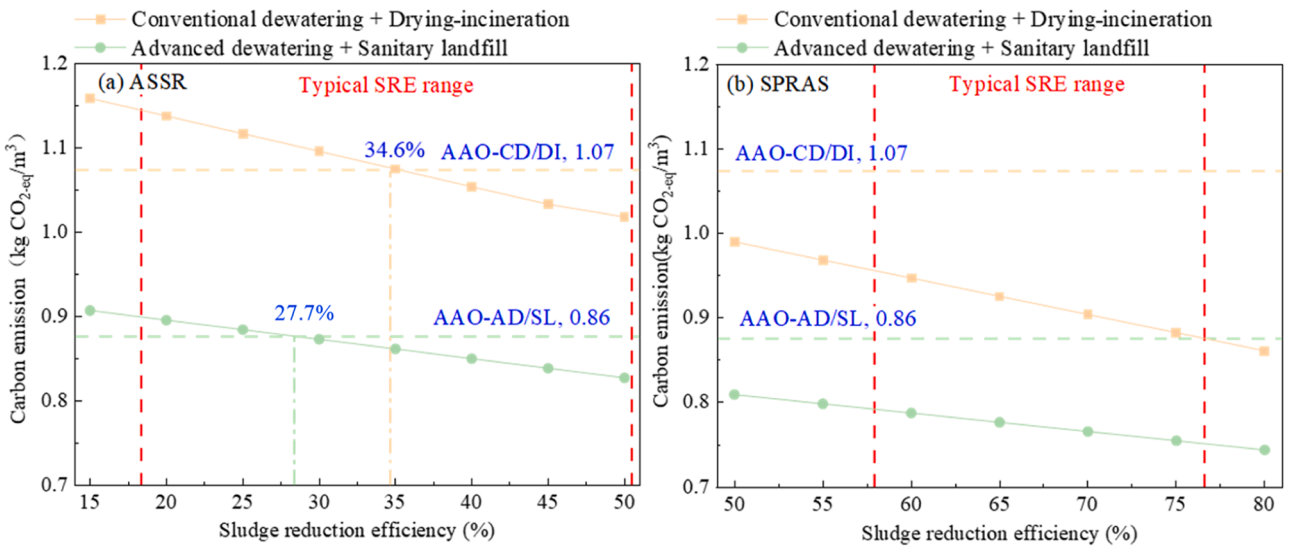

Fig. 5. Effects of sludge reduction efficiencies on GHG emissions of two SIR processes.

cost-effective technologies to reduce their carbon footprints for practical applications.

Conclusions

The carbon footprints of two typical SIR processes, ASSR and SPRAS, were evaluated with the combination of wastewater and sludge treatment systems. The results showed that compared to the AAO, the ASSR with a typical SRE of 30 % increased GHG emissions by 1.1 - 1.7 %, while the SPRAS with the SRE of 74 % reduced GHG emissions by 12.3 - 17.6 %. Electricity consumption (0.025 - 0.027 kg $CO_{2\text{-eq}}/m^3$), CO_2 (0.016 - 0.059 kg $CO_{2\text{-eq}}/m^3$), and N_2O emissions (0.009 - 0.023 kg $CO_{2\text{-eq}}/m^3$) for the removal of secondary substrates released from sludge decay in the SIR processes were the major contributor to the increased GHG emissions from the wastewater treatment system. The SIR processes greatly reduced GHG footprints of sludge treatment and disposal by decreasing sludge production and organic matter contents in the sludge. GHG emissions of SIR processes have a near linear relationship with SRE, and the threshold SREs of the ASSR for GHG reduction were 27.7 % and 34.6 % for the AD/SL and CD/DI routes, respectively. Upgrading the conventional activated sludge process to the SPRAS process created significant benefits to GHG reduction.

Materials and methods

Full-scale SIR WWTPs

The full-scale ASSR system is located at Langxia WWTP (Shanghai, China) with treatment capacity of 20,000 m^3/d (Fig. 2a). The wastewater was treated by the ASSR coupled with AAO process, followed by a submerged flat-sheet MBR for efficient solid-liquid separation. The HRTs of the ASSR, anaerobic, anoxic, aerobic, and MBR were 11.2, 2.8, 8.7, 4.7, and 3.9 h, respectively. The dissolved oxygen level in the aerobic tank was controlled at 2.0 mg/L by fine-pore diffusers. In MBR, the flat-sheet membranes were made of polyvinylidene fluoride with the mean pore size of 0.2 μm, and the membrane flux was controlled at 15 L/(m^2·h). The return activated sludge ratio was 550 % and nitrate recirculation ratio was 130 %. The ratio of sludge recirculation from the aerobic tank to the ASSR tank was 100 %. The concentration of mixed liquor suspended solids (MLSS) was maintained at 15.0 g/L, and the SRT was 30 d by discharging sludge from the MBR tank.

The full-scale SPRAS system is located at Lin'an WWTP (Zhejiang, China) with treatment capacity of 60,000 m^3/d and divided into three independent and identical subsystems (Fig. 2b). The wastewater was treated by an SPR module, a separate anaerobic unit, a triple oxidation ditch, and constructed wetlands successively. The SPR module consisted of a microaerobic tank and a settler with HRTs of 1.5 and 3.0 h, respectively. The HRTs of the anaerobic units and three-ditch oxidation ditch were 3.2, and 8.5 h, respectively. The dissolved oxygen levels in the microaerobic and aerobic tanks were controlled at 0.5 and 2.0 mg/L by fine-pore diffusers. The return activated sludge ratio was 200 % and nitrate recirculation ratio was 100 %. The ratio of sludge recirculation from the SPR settler to the microaerobic tank was 50 %. The MLSS was 4.5 g/L, and the SRT was 75 d

Data scope and scenario

Hypothetical wastewater treatment process and operation conditions

A 100,000 m^3/d WWTP supplied by domestic wastewater was used for the scenario study. Two SIR processes, ASSR and SPRAS, and a conventional AAO process were adopted as the biological treatment processes. For these three processes to achieve the Grade 1A level of the Discharge Standard of Pollutants for Municipal WWTPs of China (GB 18,918 - 2002), chemical coagulation, settling, and filtration units were used as tertiary treatment.

The AAO process was employed as the control group (Fig. 1). The HRT of anaerobic, anoxic, and aerobic tanks of the AAO was 2.0, 4.0, and 7.0 h, respectively. An ASSR and an anoxic - oxic (AO) made up the ASSR system. Anoxic, aerobic, and ASSR tanks had HRTs of 4.0, 8.0, and 6.0 h, correspondingly. A SPR and an AO unit make up the SPRAS system. The HRTs of the microaerobic tank and the settler in the SPR unit were 1.5 and 3.0 h, and those of the anoxic and aerobic tank were 4.0 and 6.0 h, respectively. The HRTs of the secondary clarifier and coagulation-settling tank in the three processes were all designed as 4.0 and 0.7 h.

In the AAO process, the MLSS were 3.0 g/L, and the SRT was 15 d In the ASSR, the MLSS concentrations of the AO and ASSR unit were 2.5 and 3.5 g/L, and the SRT was 30 d The SRT of the entire SPRAS was 80 d, and the MLSS concentrations of the SPR and AO units were kept at 6.5 and 2.5 g/L, respectively. Through the discharge of WAS into the SPR unit, the AO unit in the SPRAS kept an SRT at 15 d The dissolved oxygen level in the aerobic tanks of the three processes was controlled at 2.0 - 4.0 mg/L by fine-pore diffusers. To obtain stable SRE, the dissolved oxygen of the microaerobic tank in the SPRAS was kept at 0.2 - 0.5 mg/L (Jiang et al., 2018). All systems had a return activated sludge ratio of 200 % and nitrate recirculation ratio of 100 %. The ratio of sludge

recirculation from the SPR settler to the microaerobic tank was 50 %. To increase the efficiency of nitrogen removal in the SPRAS process, 70 % of the influent was delivered straight into the anoxic tank and bypassed the SPR unit (Zhou et al., 2014b).

Sludge treatment and disposal routes

Anaerobic digestion followed by land utilization was commonly employed in European and American countries for sludge stabilization and resource recovery; however, anaerobic digestion was not appropriate for sludge with low organic matter content (Zhou et al., 2023), which is very common in China and the WAS discharged from the SIR process. Therefore, CD/DI (Fig. 1d) and AD/SL (Fig. 1e), two typical routes for sludge treatment and disposal (Wei et al., 2020), were adopted for three processes.

Large amounts of WAS and minor amounts of chemical sludge (CS) will be produced by the wastewater treatment system; nevertheless, the effectiveness of sludge treatment and disposal will not be impacted by the combination of the two. The VSS/SS ratios of WAS in the AAO, ASSR, and SPRAS processes are 0.60, 0.55, and 0.50, respectively, according to full-scale data (Jiang et al., 2018). These ratios had a profound effect on the dosage of sludge conditioners and the subsequent biological source GHG emissions. In the route of CD/DI, the sludge was dewatered to water content of 80 % after conditioned by polyacrylamide (PAM), and then dried to water content of 30 % for incineration. The dosages of PAM were 3.50, 3.00, and 2.50 g/kg DS for the conditioning of sludge from the AAO, ASSR, and SPRAS (Zhao et al., 2020). In the AD/SL route, the sludge cake was landfilled without methane collection after being conditioned by $FeCl_3$ and lime and dewatered to a water content of 60 %. The dosages of $FeCl_3$ were 44.0, 40.3, and 36.7 g/kg DS for sludge from the AAO, ASSR, and SPRAS, with the dosage of lime fixed at 100 g/kg DS (Wu et al., 2019). It is assumed that the dewatered sludge was transported by truck for 50 km.

System boundary and GHG emission model

The system boundary of GHG emissions assessment included the wastewater treatment system (from influent to effluent) and the sludge treatment and disposal system. Both direct and indirect emissions were included in the GHG emissions, which were then expressed as carbon dioxide equivalent per m^3 of wastewater treated ($CO_{2\text{-eq}}/m^3$). Uncontrolled releases of CO_2, CH_4, and N_2O were the direct sources of GHG emissions; electricity consumption and chemical usage were the indirect sources. The carbon footprint analysis adopts and learns from the data and methods of relevant literature (Delre et al., 2019; He et al., 2023; Wang et al., 2023), which is mainly presented in supporting information. For the wastewater treatment system, the direct emissions model was constructed based on microbial kinetics and mass balances of five sub-processes, while the indirect emissions were estimated by emission factor (EF) (Table S1). GHG emissions of four key units for the sludge treatment and disposal system were determined by carefully weighing direct and indirect emissions from literatures (Wei et al., 2020; Yang et al., 2015). Next, using the developed model as a guide, the total equivalent CO_2 emissions produced in the three processes were determined.

Direct emissions of GHGs from wastewater treatment process

The direct emissions of GHGs in the five sub-processes (Table S1) mainly comes from four biochemical reactions: a) CO_2 generated from aerobic and anoxic sludge decay (GHG_{DE}, kg $CO_{2\text{-eq}}/m^3$); b) methanogenesis from anaerobic sludge decay; c) organic matter oxidation (GHG_{BOD}, kg $CO_{2\text{-eq}}/m^3$); d) nitrification and denitrification (N/DN) (GHG_{CO2} and GHG_{N2O}, kg $CO_{2\text{-eq}}/m^3$) (Ferrentino et al., 2015; Monteith et al., 2005; Nguyen et al., 2019; Pehlivanoglu-Mantas and Sedlak, 2008; Wang et al., 2011; Zhou et al., 2023). The methanogenesis from anaerobic sludge decay were not consider in this study because methane emission was at a very low level for the three processes (Text S2).

$$\mathrm{GHGDE} = \mathrm{EFDE} \times M\mathrm{DE} / Q \quad (1)$$

$$\mathrm{GHGBOD} = R\mathrm{O2} \times \mathrm{EFBOD} \quad (2)$$

$$\mathrm{GHGCO2} = \mathrm{EFN} \times M\mathrm{nitro} / Q \quad (3)$$

$$\mathrm{GHGN2O} = \mathrm{GWPN2O} \times M\mathrm{N2O} / Q \quad (4)$$

where Q is wastewater flow rate, m^3/d; R_{O2} is Net biomass oxygen consumption, kg O_2/d; M_{DE} is mass of decayed sludge, kg VSS/d; M_{nitro} and M_{N2O} are the CO_2 produced from mass of nitrogen nitrated, N_2O mass generated from N/DN, kg/d.

Indirect emissions of wastewater treatment systems

Indirect GHG emissions of energy consumption (GHG_E, kg $CO_{2\text{-eq}}/m^3$) for wastewater treatment was calculated based on CO_2 emissions per unit of energy in the area where the WWTP was located (Zhou et al., 2015b). The energy consumption of aeration mainly applies to oxygen supply for the aerobic tank and the microaerobic tank in the SPRAS. At this stage, aeration calculation adopts the blower energy consumption model proposed by Jiang et al. (2017).

The major chemical consumption in the wastewater treatment system was coagulant, which was added into the coagulation-settling tank to remove SS and residual phosphorus from the effluent of biological treatment processes. Poly aluminum chloride (PAC) of 10 mg/L and 1.25 mg/L were added to reduce TP and SS of 1 mg/L, respectively (Lucena-Silva et al., 2019), and the dosage of PAM was estimated at 5 % of PAC dosage (Aguilar et al., 2002). Indirect GHG emissions of chemical consumption (GHG_{CHE}, kg $CO_{2\text{-eq}}/m^3$) were calculated by Eq. (6).

$$\mathrm{GHGE} = E\mathrm{tot} \times \mathrm{EFE} \quad (5)$$

$$\mathrm{GHG_{CHE}} = \mathrm{EF_{CHE}} \times M_{\mathrm{CHE}} / Q \quad (6)$$

where E_{tot} is energy consumption, kWh/d; M_{CHE} is the dosing mass of chemical, kg/d.

GHG emissions from sludge treatment and disposal

The WAS produced (DS_{WAS}, kg DS/d) is calculated by COD concentrations and Y_{obs}. The CS (DS_{CS}, kg DS/d) from the coagulation-settling tank consists of coagulated SS, aluminum phosphate, and aluminum hydroxide; therefore, VSS/SS ratios in the CS of AAO, ASSR, and SPRAS were calculated as 0.29, 0.36, and 0.16, respectively, considering initial VSS/SS ratio in the effluent of biological treatment processes and the dosage of coagulant.

GHG_S (kg $CO_{2\text{-eq}}/m^3$) are GHG emissions generated from sludge treatment and disposal.

$$\mathrm{GHGS} = (\mathrm{DSWAS} \times \mathrm{EFWAS} + \mathrm{DSCS} \times \mathrm{EFCS}) / Q \quad (7)$$

where EF_{WAS} and EF_{CS} are the EFs of sludge treatment and disposal routes for WAS and CS, kg $CO_{2\text{-eq}}$/kg DS, respectively. The EF values above all are listed in Table S2.

$$\mathrm{GHG} = \mathrm{GHGDE} + \mathrm{GHGBOD} + \mathrm{GHGCO2} + \mathrm{GHGN2O} + \mathrm{GHGE} + \mathrm{GHGCHE} + \mathrm{GHGS} \quad (8)$$

where GHG is GHG emissions generated from wastewater treatment and sludge treatment and disposal, kg $CO_{2\text{-eq}}/m^3$. Detailed information on equations and relevant parameters can be found in the Supplementary information.

CRediT authorship contribution statement

Yiyue Sun: Writing – original draft, Supervision, Conceptualization.

Yi Zuo: Writing – original draft, Methodology, Data curation. **Yanjun Shao:** Writing – review & editing, Formal analysis. **Lihua Wang:** Resources. **Lu-Man Jiang:** Investigation. **Jiaming Hu:** Data curation. **Chuanting Zhou:** Supervision, Formal analysis. **Xi Lu:** Resources. **Song Huang:** Data curation. **Zhen Zhou:** Writing – review & editing, Supervision, Data curation.

Declaration of competing interest

The authors declare that they have no known competing financial interests or personal relationships that could have appeared to influence the work reported in this paper.

Data availability

Data will be made available on request

Acknowledgments

This work was supported by the National Natural Science Foundation of China (51878403), the Shanghai Outstanding Academic Leaders Plan (23XD1421300), the Science and Technology Commission of Shanghai Municipality of China (22DZ1209206), and the Research Project of Shanghai Investigation Design and Research Institute Co., Ltd. (2021SZ (8)−003).

Supplementary materials

Supplementary material associated with this article can be found, in the online version, at doi:10.1016/j.wroa.2024.100243.

References

Aguilar, M.I., Sáez, J., Lloréns, M., Soler, A., Ortuño, J.F., 2002. Nutrient removal and sludge production in the coagulation-flocculation process. Water Res. 36 (11), 2910–2919. https://doi.org/10.1016/S0043-1354(01)00508-5.

An, Y., Zhou, Z., Yao, J., Niu, T., Qiu, Z., Ruan, D., Wei, H., 2017. Sludge reduction and microbial community structure in an anaerobic/anoxic/oxic process coupled with potassium ferrate disintegration. Bioresour. Technol. 245, 954–961. https://doi.org/10.1016/j.biortech.2017.09.023.

Bani Shahabadi, M., Yerushalmi, L., Haghighat, F., 2009. Impact of process design on greenhouse gas (GHG) generation by wastewater treatment plants. Water Res. 43 (10), 2679–2687. https://doi.org/10.1016/j.watres.2009.02.040.

Bani Shahabadi, M., Yerushalmi, L., Haghighat, F., 2010. Estimation of greenhouse gas generation in wastewater treatment plants-Model development and application. Chemosphere 78 (9), 1085–1092. https://doi.org/10.1016/j.chemosphere.2009.12.044.

Brown, S., Beecher, N., Carpenter, A., 2010. Calculator tool for determining greenhouse gas emissions for biosolids processing and end use. Environ. Sci. Technol. 44 (24), 9509–9515. https://doi.org/10.1021/es101210k.

Chen, W., Liu, J., Zhu, B.-H., Shi, M.-Y., Zhao, S.-Q., He, M.-Z., Yan, P., Fang, F., Guo, J.-S., Li, W., Chen, Y.-P., 2022. The GHG mitigation opportunity of sludge management in China. Environ. Res. 212, 113284 https://doi.org/10.1016/j.envres.2022.113284.

Cheng, C., Zhou, Z., Niu, T., An, Y., Shen, X., Pan, W., Chen, Z., Liu, J., 2017. Effects of side-stream ratio on sludge reduction and microbial structures of anaerobic side-stream reactor coupled membrane bioreactors. Bioresour. Technol. 234, 380–388. https://doi.org/10.1016/j.biortech.2017.03.077.

Cheng, C., Zhou, Z., Pang, H., Zheng, Y., Chen, L., Jiang, L.-M., Zhao, X., 2018. Correlation of microbial community structure with pollutants removal, sludge reduction and sludge characteristics in micro-aerobic side-stream reactor coupled membrane bioreactors under different hydraulic retention times. Bioresour. Technol. 260, 177–185. https://doi.org/10.1016/j.biortech.2018.03.088.

Delre, A., ten Hoeve, M., Scheutz, C., 2019. Site-specific carbon footprints of Scandinavian wastewater treatment plants, using the life cycle assessment approach. J. Clean. Prod. 211, 1001–1014. https://doi.org/10.1016/j.jclepro.2018.11.200.

Fan, H., Qi, L., Liu, G., Zhang, Y., Fan, Q., Wang, H., 2017. Aeration optimization through operation at low dissolved oxygen concentrations: evaluation of oxygen mass transfer dynamics in different activated sludge systems. J. Environ. Sci. 55, 224–235. https://doi.org/10.1016/j.jes.2016.08.008.

Ferrentino, R., Langone, M., Andreottola, G., 2019. Progress toward full scale application of the anaerobic side-stream reactor (ASSR) process. Bioresour. Technol. 272, 267–274. https://doi.org/10.1016/j.biortech.2018.10.028.

Ferrentino, R., Langone, M., Merzari, F., Tramonte, L., Andreottola, G., 2015. A review of anaerobic side-stream reactor for excess sludge reduction: configurations, mechanisms, and efficiency. Critical Rev. Environ. Sci. Technol. 46 (4), 382–405. https://doi.org/10.1080/10643389.2015.1096879.

Flores-Alsina, X., Arnell, M., Amerlinck, Y., Corominas, L., Gernaey, K.V., Guo, L., Lindblom, E., Nopens, I., Porro, J., Shaw, A., Snip, L., Vanrolleghem, P.A., Jeppsson, U., 2014. Balancing effluent quality, economic cost and greenhouse gas emissions during the evaluation of (plant-wide) control/operational strategies in WWTPs. Sci. Total Environ. 466-467, 616–624. https://doi.org/10.1016/j.scitotenv.2013.07.046.

Flores-Alsina, X., Corominas, L., Snip, L., Vanrolleghem, P.A., 2011. Including greenhouse gas emissions during benchmarking of wastewater treatment plant control strategies. Water Res. 45 (16), 4700–4710. https://doi.org/10.1016/j.watres.2011.04.040.

Foley, J., de Haas, D., Yuan, Z., Lant, P., 2010. Nitrous oxide generation in full-scale biological nutrient removal wastewater treatment plants. Water Res. 44 (3), 831–844. https://doi.org/10.1016/j.watres.2009.10.033.

Gu, Y., Dong, Y.-n, Wang, H., Keller, A., Xu, J., Chiramba, T., Li, F., 2016. Quantification of the water, energy and carbon footprints of wastewater treatment plants in China considering a water-energy nexus perspective. Ecol. Indic. 60, 402–409. https://doi.org/10.1016/j.ecolind.2015.07.012.

He, X., Li, Z., Xing, C., Li, Y., Liu, M., Gao, X., Ding, Y., Lu, L., Liu, C., Li, C., Wang, D., 2023. Carbon footprint of a conventional wastewater treatment plant: an analysis of water-energy nexus from life cycle perspective for emission reduction. J. Clean. Prod. 429, 139562 https://doi.org/10.1016/j.jclepro.2023.139562.

Huang, F., Shen, W., Zhang, X., Seferlis, P., 2020a. Impacts of dissolved oxygen control on different greenhouse gas emission sources in wastewater treatment process. J. Clean. Prod. 274, 123233 https://doi.org/10.1016/j.jclepro.2020.123233.

Huang, H., Ekama, G.A., Biswal, B.K., Dai, J., Jiang, F., Chen, G.-H., Wu, D., 2019. A new sulfidogenic oxic-settling anaerobic (SOSA) process: the effects of sulfur-cycle bioaugmentation on the operational performance, sludge properties and microbial communities. Water Res. 162, 30–42. https://doi.org/10.1016/j.watres.2019.06.051.

Huang, J., Zhou, Z., Zheng, Y., Sun, X., Yu, S., Zhao, X., Yang, A., Wu, C., Wang, Z., 2020b. Biological nutrient removal in the anaerobic side-stream reactor coupled membrane bioreactors for sludge reduction. Bioresour. Technol. 295, 122241 https://doi.org/10.1016/j.biortech.2019.122241.

Huang, Y., Meng, F., Liu, S., Sun, S., Smith, K., 2023. China's enhanced urban wastewater treatment increases greenhouse gas emissions and regional inequality. Water Res. 230, 119536 https://doi.org/10.1016/j.watres.2022.119536.

Jiang, J., Zhou, Z., Jiang, L., Zheng, Y., Zhao, X., Chen, G., Wang, M., Huang, J., An, Y., Wu, Z., 2021. Bacterial and microfauna mechanisms for sludge reduction in carrier-enhanced anaerobic side-stream reactors revealed by metagenomic sequencing analysis. Environ. Sci. Technol. 55 (9), 6257–6269. https://doi.org/10.1021/acs.est.0c07880.

Jiang, L.-M., Garrido-Baserba, M., Nolasco, D., Al-Omari, A., DeClippeleir, H., Murthy, S., Rosso, D., 2017. Modelling oxygen transfer using dynamic alpha factors. Water Research 124, 139–148. https://doi.org/10.1016/j.watres.2017.07.032.

Jiang, L.-M., Zhou, Z., Cheng, C., Li, J., Huang, C., Niu, T., 2018. Sludge reduction by a micro-aerobic hydrolysis process: a full-scale application and sludge reduction mechanisms. Bioresour. Technol. 268, 684–691. https://doi.org/10.1016/j.biortech.2018.08.070.

Li, Q., Xu, Y., Liang, C., Peng, L., Zhou, Y., 2023. Nitrogen removal by algal-bacterial consortium during mainstream wastewater treatment: transformation mechanisms and potential N_2O mitigation. Water Res. 235, 119890 https://doi.org/10.1016/j.watres.2023.119890.

Lu, L., Guest, J.S., Peters, C.A., Zhu, X., Rau, G.H., Ren, Z.J., 2018. Wastewater treatment for carbon capture and utilization. Nature Sustainability 1 (12), 750–758. https://doi.org/10.1038/s41893-018-0187-9.

Lucena-Silva, D.d., Molozzi, J., Severiano, J.d.S., Becker, V., Lucena Barbosa, J.E.d., 2019. Removal efficiency of phosphorus, cyanobacteria and cyanotoxins by the "flock & sink" mitigation technique in semi-arid eutrophic waters. Water Res. 159, 262–273. https://doi.org/10.1016/j.watres.2019.04.057.

Mannina, G., Rebouças, T.F., Cosenza, A., Chandran, K., 2019. A plant-wide wastewater treatment plant model for carbon and energy footprint: model application and scenario analysis. J. Clean. Prod. 217, 244–256. https://doi.org/10.1016/j.jclepro.2019.01.255.

Menéndez, J.A., Inguanzo, M., Pis, J.J., 2002. Microwave-induced pyrolysis of sewage sludge. Water Res. 36 (13), 3261–3264. https://doi.org/10.1016/S0043-1354(02)00017-9.

Monteith, H.D., Sahely, H.R., Maclean, H.L., Bagley, D.M., 2005. A rational procedure for estimation of greenhouse-gas emissions from municipal wastewater treatment plants. Water Environ. Res. 77 (4), 390–403. https://doi.org/10.1002/j.1554-7531.2005.tb00298.x.

Nayeb, H., Mirabi, M., Motiee, H., Alighardashi, A., Khoshgard, A., 2019. Estimating greenhouse gas emissions from Iran's domestic wastewater sector and modeling the emission scenarios by 2030. J. Clean. Prod. 236, 117673 https://doi.org/10.1016/j.jclepro.2019.117673.

Nguyen, T.K.L., Ngo, H.H., Guo, W., Chang, S.W., Nguyen, D.D., Nghiem, L.D., Liu, Y., Ni, B., Hai, F.I., 2019. Insight into greenhouse gases emissions from the two popular treatment technologies in municipal wastewater treatment processes. Sci. Total Environ. 671, 1302–1313. https://doi.org/10.1016/j.scitotenv.2019.03.386.

Niu, T., Zhou, Z., Shen, X., Qiao, W., Jiang, L.-M., Pan, W., Zhou, J., 2016. Effects of dissolved oxygen on performance and microbial community structure in a micro-aerobic hydrolysis sludge in situ reduction process. Water Res. 90, 369–377. https://doi.org/10.1016/j.watres.2015.12.050.

Pagilla, K., Shaw, A., Kunetz, T., Schiltz, M., 2009. A systematic approach to establishing carbon footprints for wastewater treatment plants. In: WEFTEC 2009. Proceedings of the Water Environment Federation, pp. 5399–5409.

Pehlivanoglu-Mantas, E., Sedlak, D.L., 2008. Measurement of dissolved organic nitrogen forms in wastewater effluents: concentrations, size distribution and NDMA formation potential. Water Res. 42 (14), 3890–3898. https://doi.org/10.1016/j.watres.2008.05.017.

Qin, Y., Wang, K., Xia, Q., Yu, S., Zhang, M., An, Y., Zhao, X., Zhou, Z., 2023. Up-concentration of nitrogen from domestic wastewater: a sustainable strategy from removal to recovery. Che. Eng. J. 451, 138789 https://doi.org/10.1016/j.cej.2022.138789.

Samuelsson, J., Delre, A., Tumlin, S., Hadi, S., Offerle, B., Scheutz, C., 2018. Optical technologies applied alongside on-site and remote approaches for climate gas emission quantification at a wastewater treatment plant. Water Res. 131, 299–309. https://doi.org/10.1016/j.watres.2017.12.018.

Shao, Y., Zhou, Z., Zuo, Y., Jiang, J., Wang, L., Sun, Y., He, J., Qiu, J., An, Y., Jiang, L.-M., 2022. Sludge decay kinetics and metagenomic analysis uncover discrepant metabolic mechanisms in two different sludge in situ reduction systems. Sci. Total Environ. 851, 158346 https://doi.org/10.1016/j.scitotenv.2022.158346.

Torregrossa, M., Di Bella, G., Di Trapani, D., 2012. Comparison between ozonation and the OSA process: analysis of excess sludge reduction and biomass activity in two different pilot plants. Water Sci. Technol. 66 (1), 185–192. https://doi.org/10.2166/wst.2012.153.

Velho, V.F., Foladori, P., Andreottola, G., Costa, R.H.R., 2016. Anaerobic side-stream reactor for excess sludge reduction: 5-year management of a full-scale plant. J. Environ. Manage. 177, 223–230. https://doi.org/10.1016/j.jenvman.2016.04.020.

Wang, J., Zhang, J., Wang, J., Qi, P., Ren, Y., Hu, Z., 2011. Nitrous oxide emissions from a typical northern Chinese municipal wastewater treatment plant. Desalinat. Water Treatm. 32 (1–3), 145–152.

Wang, S., Li, X., Ji, M., Zhang, J., Tanveer, M., Hu, Z., 2023. Is constructed wetlands carbon source or carbon sink? Case analysis based on life cycle carbon emission accounting. Bioresour. Technol. 388, 129777 https://doi.org/10.1016/j.biortech.2023.129777.

Wang, Z., Yu, H., Ma, J., Zheng, X., Wu, Z., 2013. Recent advances in membrane bio-technologies for sludge reduction and treatment. Biotechnol. Adv. 31 (8), 1187–1199. https://doi.org/10.1016/j.biotechadv.2013.02.004.

Wei, L., Zhu, F., Li, Q., Xue, C., Xia, X., Yu, H., Zhao, Q., Jiang, J., Bai, S., 2020. Development, current state and future trends of sludge management in China: based on exploratory data and CO_2-equivaient emissions analysis. Environ Int 144, 106093. https://doi.org/10.1016/j.envint.2020.106093.

Wu, W., Zhou, Z., Yang, J., Chen, G., Yao, J., Tu, C., Zhao, X., Qiu, Z., Wu, Z., 2019. Insights into conditioning of landfill sludge by FeCl3 and lime. Water Res. 160, 167–177. https://doi.org/10.1016/j.watres.2019.05.071.

Yang, G., Zhang, G., Wang, H., 2015. Current state of sludge production, management, treatment and disposal in China. Water Res. 78, 60–73. https://doi.org/10.1016/j.watres.2015.04.002.

Zhao, X., Jiang, J., Zhou, Z., Yang, J., Chen, G., Wu, W., Sun, D., Yao, J., Qiu, Z., He, K., Wu, Z., Lou, Z., 2020. Applying organic polymer flocculants in conditioning and advanced dewatering of landfill sludge as a substitution of ferric trichloride and lime: mechanism, optimization and pilot-scale study. Chemosphere 260, 127617. https://doi.org/10.1016/j.chemosphere.2020.127617.

Zheng, Y., Cheng, C., Zhou, Z., Pang, H., Chen, L., Jiang, L.-M., 2019a. Insight into the roles of packing carriers and ultrasonication in anaerobic side-stream reactor coupled membrane bioreactors: sludge reduction performance and mechanism. Water Res 155, 310–319. https://doi.org/10.1016/j.watres.2019.02.039.

Zheng, Y., Zhou, Z., Ye, X., Huang, J., Jiang, L., Chen, G., Chen, L., Wang, Z., 2019b. Identifying microbial community evolution in membrane bioreactors coupled with anaerobic side-stream reactor, packing carriers and ultrasonication for sludge reduction by linear discriminant analysis. Bioresour. Technol. 291, 121920 https://doi.org/10.1016/j.biortech.2019.121920.

Zhou, X., Yang, J., Zhao, X., Dong, Q., Wang, X., Wei, L., Yang, S.-S., Sun, H., Ren, N.-Q., Bai, S., 2023a. Towards the carbon neutrality of sludge treatment and disposal in China: a nationwide analysis based on life cycle assessment and scenario discovery. Environ Int 174, 107927. https://doi.org/10.1016/j.envint.2023.107927.

Zhou, Z., Qiao, W., Xing, C., Shen, X., Hu, D., Wang, L., 2014a. A micro-aerobic hydrolysis process for sludge in situ reduction: performance and microbial community structure. Bioresour. Technol. 173, 452–456. https://doi.org/10.1016/j.biortech.2014.09.119.

Zhou, Z., Qiao, W., Xing, C., Wang, C., Jiang, L.-M., Gu, Y., Wang, L., 2015a. Characterization of dissolved organic matter in the anoxic-oxic-settling-anaerobic sludge reduction process. Chem. Eng. J. 259, 357–363. https://doi.org/10.1016/j.cej.2014.07.129.

Zhou, Z., Qiao, W., Xing, C., Wang, Y., Wang, C., 2014b. Sludge reduction and performance analysis of a modified sludge reduction process. Water Sci. Technol. 69 (5), 934–940. https://doi.org/10.2166/wst.2013.797.

Zhou, Z., Shen, X., Jiang, L.-M., Wu, Z., Wang, Z., Ren, W., Hu, D., 2015b. Modeling of multimode anaerobic/anoxic/aerobic wastewater treatment process at low temperature for process optimization. Chem. Eng. J. 281, 644–650. https://doi.org/10.1016/j.cej.2015.07.017.

Zhou, Z., Sun, Y., Fu, L., Zuo, Y., Shao, Y., Wang, L., Zhou, C., An, Y., 2023b. Unraveling roles of the intermediate settler in a microaerobic hydrolysis sludge in situ reduction process. Bioresour. Technol. 384, 129228 https://doi.org/10.1016/j.biortech.2023.129228.